Figure S1. Protein expression levels of oxidative stress, inflammation, fibrotic and insulin regulatory biomarkers following treatment with p-Cresol and dulaglutide. (A) Protein expression levels were detected by western blot analysis. Semi-quantification of (B) NOX-1, (C) GLP-1, (D) TGF-β, (E) NOX-2, (F) MMP-9, (G) p-Smad3/Smad3, (H) TNF-α, (I) IL-1β, (J) DPP4, (K) Nrf2, (L) GLP-1R and (M) NQO-1. All statistical analyses were performed by one-way ANOVA, followed by Bonferroni's multiple comparisons post hoc test. Data are representative of three independent experiments (n=3). $^{\#}$P<0.05 vs. Group A1; $^{*}$P<0.05, $^{**}$P<0.01 vs. Group A2. DPP4, dipeptidyl peptidase 4; GLP-1, glucagon-like peptide 1; GLP-1R, GLP-1 receptor; NQO-1, NAD(P)H quinone oxidoreductase 1; Nrf2, nuclear factor erythroid 2-related factor 2; p-, phosphorylated.

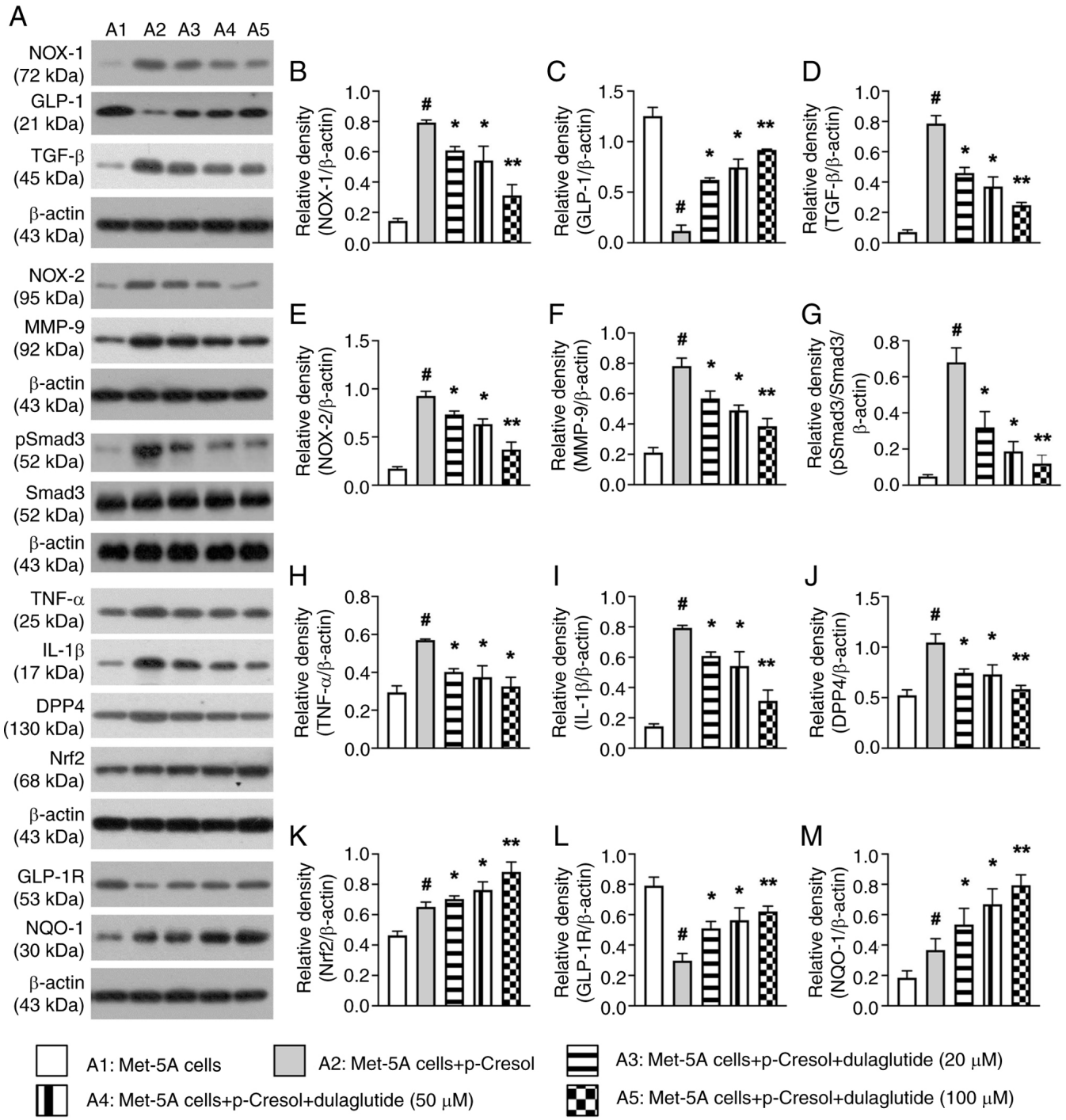

Figure S2. Impact of dulaglutide therapy on regulating cell viability, ROS generation, and early and late apoptosis following p-Crestol stimulation. Cell viability at (A) 24, (B) 48 and (C) 72 h was detected using the MTT assay. (D) Flow cytometric analysis was performed to identify total intracellualr ROS levels. (E) Total intracellular ROS levels at 72 h. (F) Flow cytometric analysis was performed to identify mitochondrial ROS. (G) Mitochondrial ROS levels at 72h. (H) Flow cytometric analysis was performed to detect cellular apoptosis. (I) Early (Annexin-V$^{+}$/PI$^{-}$) and (J) late (Annexin-V$^{+}$/PI$^{+}$) apoptosis levels. All statistical analyses were performed by one-way ANOVA, followed by Bonferroni's multiple comparisons post hoc test. Data are representative of four independent experiments (n=4). $^{\#}$P<0.05 vs. Group B1; $^{*}$P<0.05 vs. Group B2. ROS, reactive oxygen species.

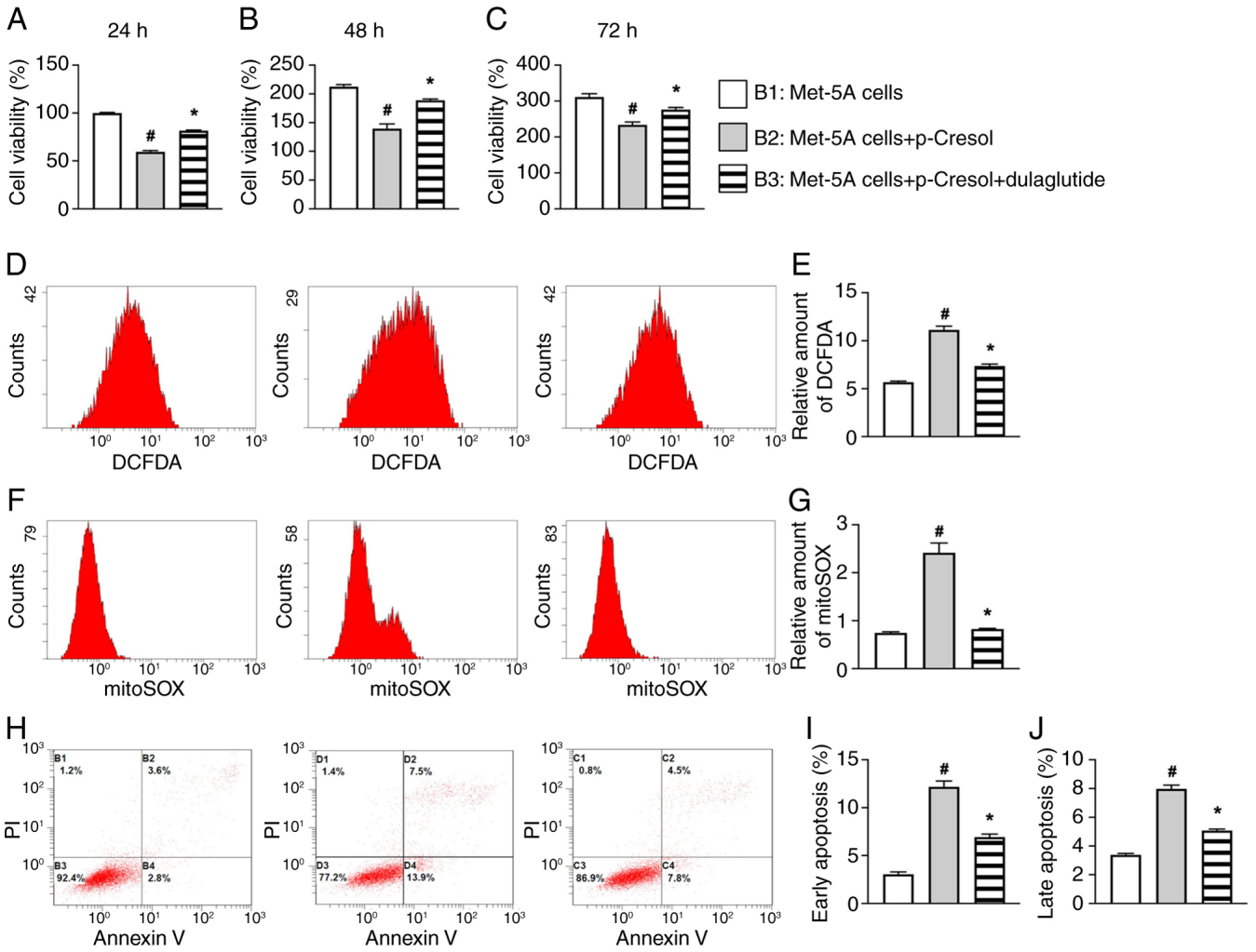

Figure S3. Impact of dulaglutide on inhibiting LPS-induced inflammatory reaction. (A) Protein expression levels were detected by western blot analysis. Semi-quantification of (B) TLR-2, (C) TLR-4, (D) NF-κB, (E) TNF and (F) MMP-9. Findings of immunofluorescence analysis (magnification, x400), which was performed to detect CD11b$^+$ cells (green). Scale bar, 20 $\mu$m. Images of (G) Met-5A cells, (H) Met-5A cells + LPS and (I) Met-5A cells + LPS + dulaglutide. (J) Number of positively stained CD11b$^+$ cells. All statistical analyses were performed by one-way ANOVA, followed by Bonferroni's multiple comparisons post hoc test. Data are representative of four independent experiments (n=4). $^{\#}$P<0.05 vs. Group C1; $^{*}$P<0.05 vs. Group C2. LPS, lipopolysaccharide; TLR, Toll-like receptor.

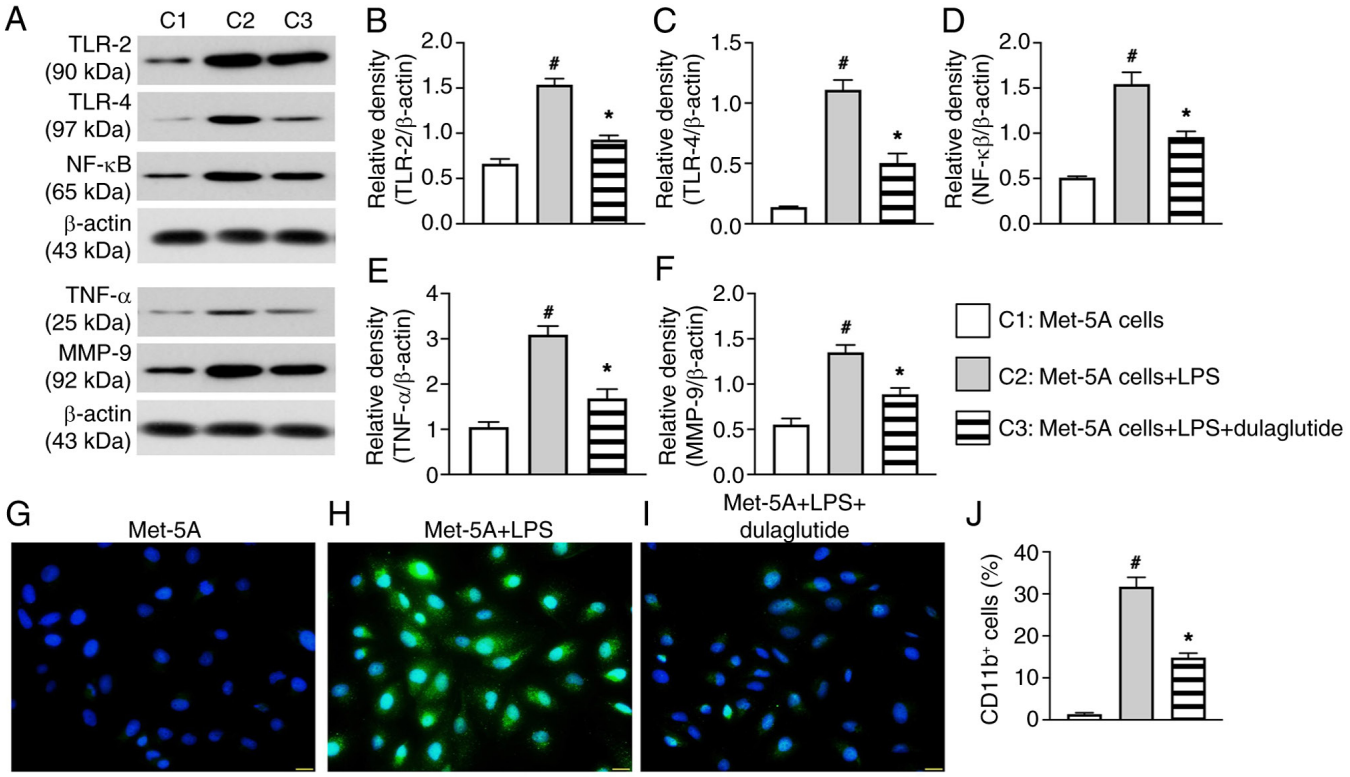

Figure S4. Verification of successful transfection. (A) Protein expression levels were detected by western blotting. Semi-quantification of (B) GLP-1, (C) vimentin, (D) NOX-1, (E) Snail, (F) NF-κB, (G) TGF-β, (H) TNF-α, (I) α-SMA, (J) p-Smad3/Smad3, (K) DPP4, (L) β-catenin and (M) NOX-2. All statistical analyses were performed by one-way ANOVA, followed by Bonferroni's multiple comparisons post hoc test (n=6/group). *P<0.05 vs. Met-5A cells + siRNA (negative control); ns, not significant. α-SMA, α-smooth muscle actin; DPP4, dipeptidyl peptidase4; GLP-1, glucagon-like peptide 1; p-, phosphorylated; siRNA, small interfering RNA.

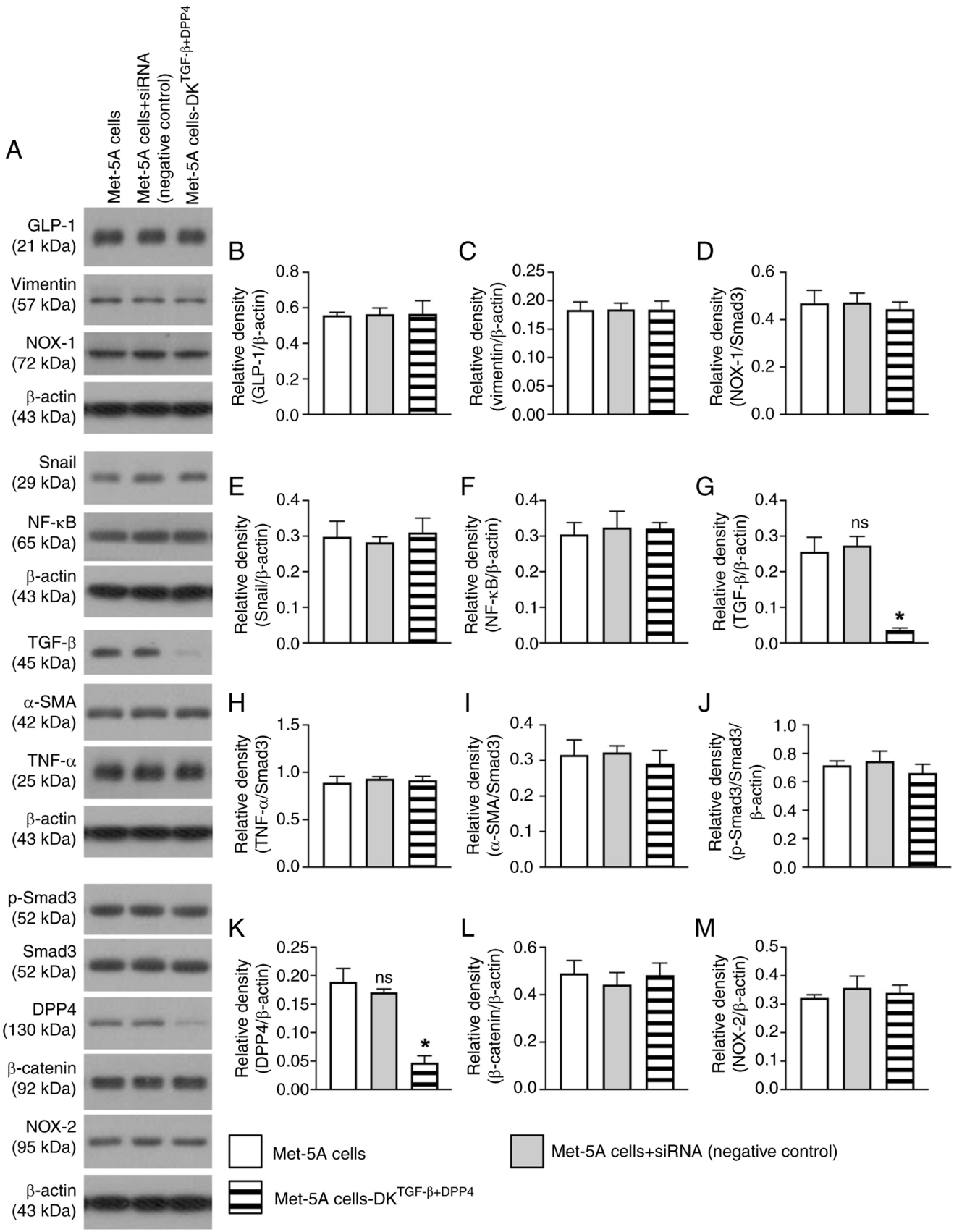

Figure S5. Unique roles of DPP4 and TFG-β in the epithelial-mesenchymal transition process and fibrosis. (A) Protein expression levels were detected by western blot analysis. Semi-quantification of (B) GLP-1, (C) vimentin, (D) NOX-2, (E) NF-κB, (F) p-Smad3/Smad3, (G) TGF-β, (H) DPP4, (I) Snail, (J) α-SMA, (K) β-catenin, (L) NOX-1 and (M) TNF-α. All statistical analyses were performed by one-way ANOVA, followed by Bonferroni's multiple comparisons post hoc test. Data are representative of six independent experiments (n=6). #P<0.05 vs. Group D1; *P<0.05 vs. Group D3. α-SMA, α-smooth muscle actin; DPP4, dipeptidyl peptidase 4; GLP-1, glucagon-like peptide 1; p-, phosphorylated.

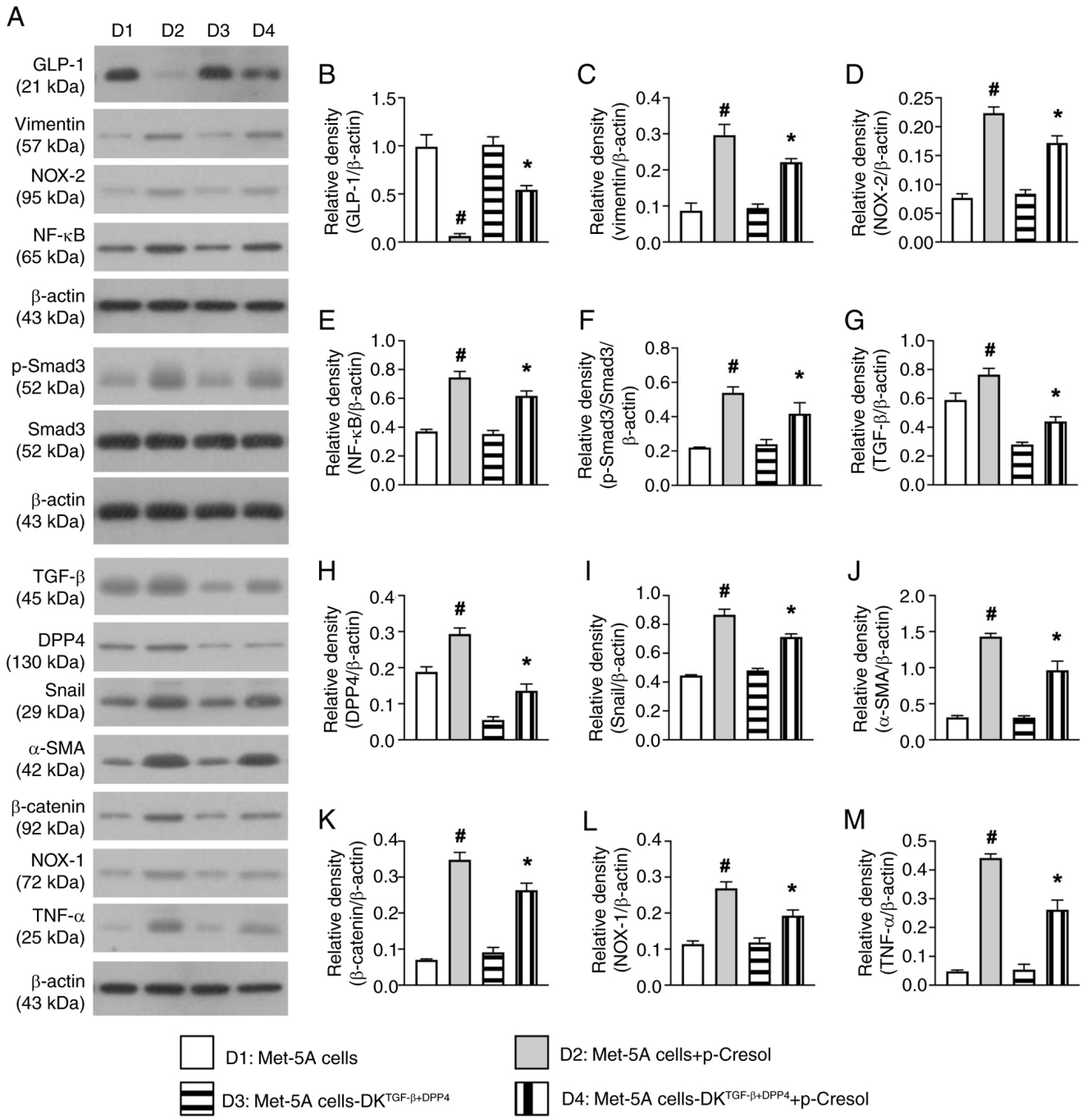

Figure S6. Expression levels of epithelial-mesenchymal transition biomarkers in Met-5A cells undergoing TGF-β and CG stimulation. (A) Protein expression levels were detected by western blot analysis. Semi-quantification of (B) p-Smad3/Smad3, (C) Snail, (D) vimentin, (E) TGF-β, (F) β-catenin, (G) α-SMA and (H) fibronectin. All statistical analyses were performed by one-way ANOVA, followed by Bonferroni's multiple comparisons post hoc test. Data are representative of three independent experiments (n=3). #P<0.05 vs. Group E1; *P<0.05 vs. Group E2; †P<0.05 vs. Group E3. α-SMA, α-smooth muscle actin; CG, chlorhexidine gluconate; p-, phosphorylated.

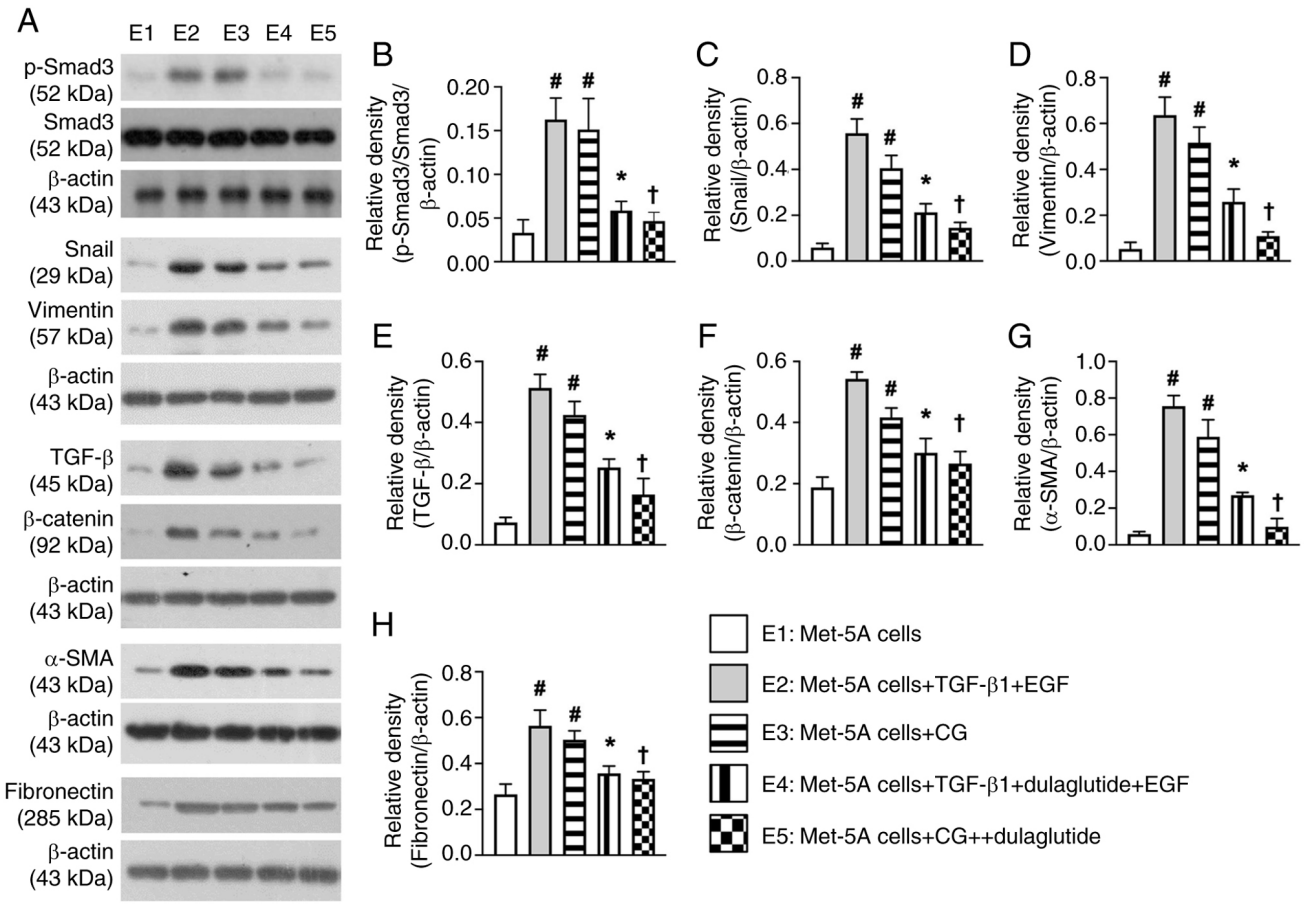

Figure S7. Phalloidin staining identifies the morphological features of the Met-5A cell cytoskeleton. Findings of immunofluorescence analysis (magnification, x200), of phalloidin staining, which was performed to identify the morphological features of the cell cytoskeleton and fluorescence intensity in Met-5A. The cytoskeleton (red arrows) was not only prominent and more crowded, but also exhibited a more typical spindle shape (indicative of mesenchymal cell morphology) in the CG-treated group than in other groups. Scale bars, 50 $\mu$m. Images of (A) Met-5A cells, (B) Met-5A cells + TGF-β1 + EGF, (C) Met-5A cells + CG, (D) Met-5A cells + TGF-β1 + EGF + dulaglutide and (E) Met-5A cells + CG + dulaglutide. (F) Cell length. (G) Number of spindle-shaped cells. (H) Mean fluorescence intensity of phalloidin staining. All statistical analyses were performed by one-way ANOVA, followed by Bonferroni's multiple comparisons post hoc test (n=5/group). $^{\#}$P<0.05 vs. Group E1; $^{*}$P<0.05 vs. Group E2; $^{\dagger}$P<0.05 vs. Group E3. CG, chlorhexidine gluconate.

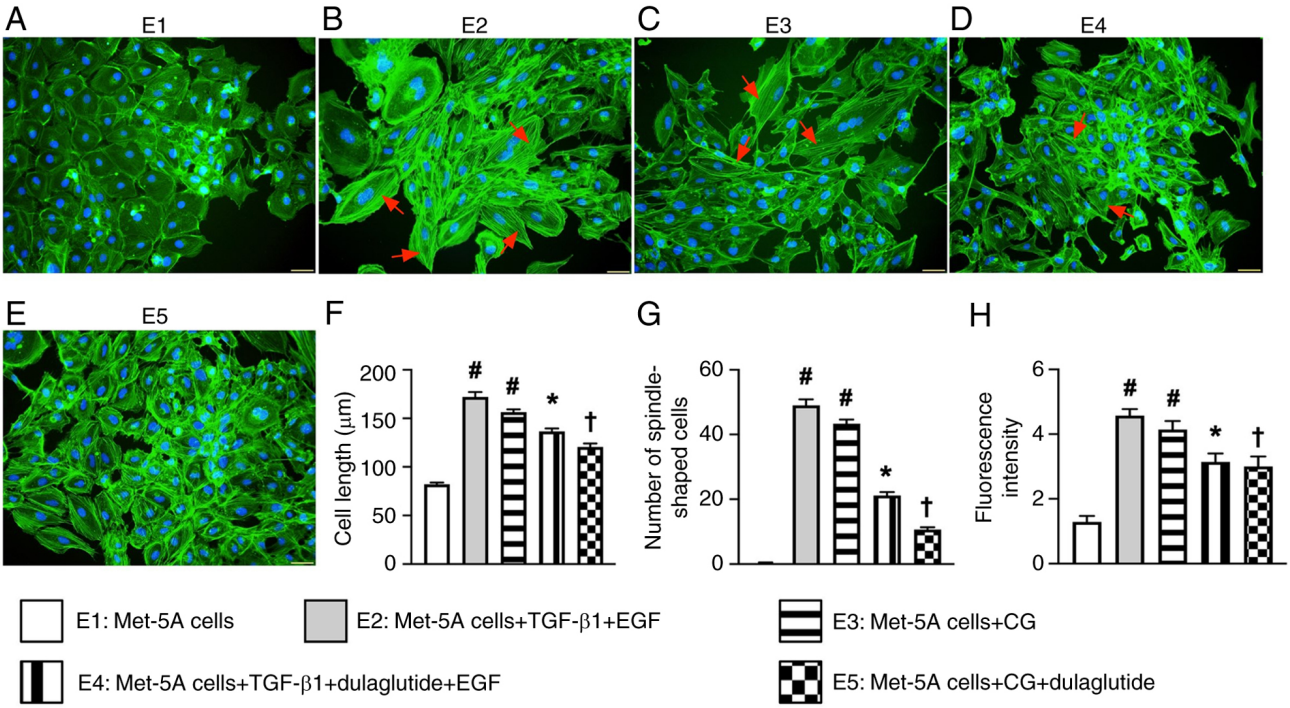

Figure S8. Time points of CKD induction, treatment and blood samplings for asessment of renal function. CG, chlorhexidine gluconate; CKD, chronic kidney disease.

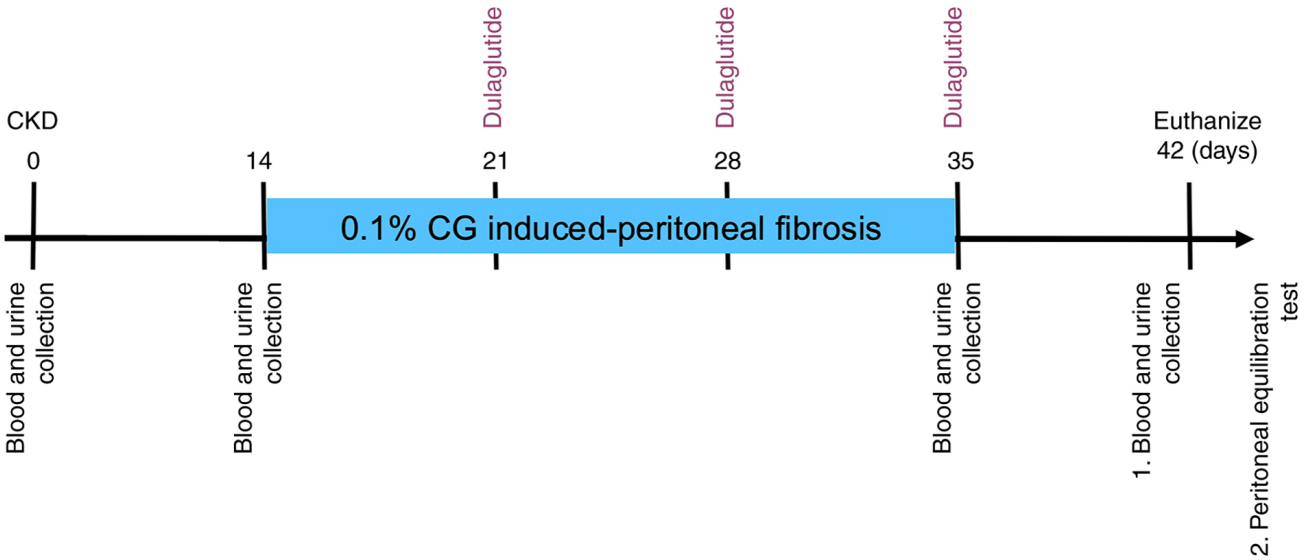

Figure S9. Flow cytometry plots. Flow cytometric analysis of the number of (A) CD11b/c$^+$, (B) MPO$^+$ and (C) Ly6G$^+$ cells in circulation. Flow cytometric analysis of the number of (D) CD11b/c$^+$, (E) MPO$^+$ and (F) Ly6G$^+$ cells in the abdominal fluid. LPS, lipopolysaccharide; MPO, myeloperoxidase; SC, sham control.